

# EVALUATION OF THE IMPULSE HAMMER TECHNIQUE FOR CORE MECHANICAL PROPERTIES PROFILING

P. Gramin<sup>1</sup>, R. Fisher<sup>1</sup>, R., A. Frooqnia<sup>1</sup>, A. Ai<sup>1</sup>, P. Hojnacki<sup>2</sup>, G. Boitnott<sup>3</sup>, L. Louis<sup>3</sup>, J. Hampton<sup>3</sup>

<sup>1</sup>BP, Houston, TX, United States

<sup>2</sup>ALS Reservoir Laboratories, Houston, TX, United States

<sup>3</sup>New England Research, Inc., White River Junction, VT, United States

*This paper was prepared for presentation at the International Symposium of the Society of Core Analysts held in Snowmass, Colorado, USA, 21-26 August 2016*

## ABSTRACT

As a part of an evaluation program conducted on several of BP's cores from deepwater Gulf of Mexico fields, a new probe was used to assess its potential as a non-destructive solution for geomechanical profiling. This mechanical probe measures the force-time relationship of a mass (referred to as Impulse Hammer) while it is freely falling onto the surface of a core from a known height. The force-time function is subsequently analyzed by an elastic Hertzian solution to obtain a reduced Young's modulus  $E^*$ , which is then used as a first-order strength indicator. Twenty one feet of slabbed core were analyzed for variations in  $E^*$  and compared with Scratch Test results. For comparison, we grouped the data into several litho-facies while each group retained a minimum number of representative data points. We observed that  $E^*$  reliably captured the variability of mechanical properties throughout the data. Results showed that the Impulse Hammer method provides a nondestructive alternative to the Scratch Test as a mechanical profiling tool. The Impulse Hammer data analysis also generates a second parameter that quantifies the deviation of core from a purely elastic behavior. Even though the use of this parameter is not thoroughly reviewed in the present study, its potential to yield a more complete picture of the core's mechanical properties and to improve the scratch test comparison is briefly discussed.

## INTRODUCTION

Historically, when a whole core is collected for analysis, some form of vertical variability characterization is used to focus on sampling locations for special core analysis (SCAL). For petrophysical SCAL, this process normally involves cutting routine core analysis (RCA) plugs at a regularly sampled interval (1.0 or 0.5 foot are common depth increments). The routine plugs are then used to determine porosity and gas permeability as storage and flow capacity parameters to be employed in SCAL sample selection. Until 2008, the process by geomechanics specialists to characterize vertical variability included the use of porosity and permeability, petrophysical rock typing, core gamma ray, and/or a log-derived rock strength [1].

Starting in 2008, Terratek (now a Schlumberger company) introduced a rock strength profiling technique, known as the Scratch Test, which has been calibrated to unconfined compressive strength (UCS) core tests [5]. This technique has proven reliable and trustworthy in characterizing vertical variability in mechanical properties and approximating unconfined compressive strength. Because the method results in the cutting of a small furrow roughly 8 mm wide by 0.2 to 2 mm deep along the core face, geologists and sedimentologists have typically been unwilling to allow this strength profiling to occur on the geologic slab due to the concerns that the process damages the core. Alternatively, the Scratch Test methodology can also be run on core butts (3/4 sections) before or after the routine core plugging process. If before, the scratch test delays the cutting of the RCA plugs, geochemistry sampling, and/or petrophysical SCAL plugs, which may be sensitive to oil-based mud invasion or mechanical degradation of the rock strength (particularly in weakly consolidated sands). If after, the Scratch Test is collected over short intervals and in between core plugs could be impacted by the removal of core material.

In 2013, a new and non-damaging strength profiling technique was introduced by New England Research (NER) onto their AutoScan platform. The technique, known as Impulse Hammer, measures the reduced Young's modulus, or  $E^*$ , by measuring the force-time response at the tip of a small instrumented sensor dropped on a core surface from a specified height and sampling interval. The technique was designed to provide a non-destructive option for mechanical profiling that can also be used to map 1 and 2D variability in mechanical properties such as elastic stiffness. To evaluate this new mechanical properties profiling process for incorporation into BP's core analysis workflows, BP worked with ALS Reservoir Laboratories (ALS) and New England Research (NER) to trial the Impulse Hammer technique on core where Scratch Test results were also available. More specifically, this study sought to answer the following questions:

- (1) Are Impulse Hammer and Scratch Test techniques consistent between each other in capturing the variations of the core mechanical properties (i.e. what level of heterogeneities is each testing platform sensitive to)?
- (2) Can empirical relationships be formulated between the rock strength index values obtained from the Scratch Test and the reduced Young's modulus  $E^*$  obtained from the Impulse Hammer?

## **MATERIALS AND METHODS**

### **Material Tested**

The material tested consists of core sections and plugs selected by BP from three different formations encountered in GoM deepwater fields. All the original sections had previously been analyzed with a Scratch Test probe. For Fields A and B, the core sections were still available for impulse hammer profiling, while plugs that had been extracted from the scratched core were used for field C. The table below provides a description of the core material.

**Table 1. Summary of tested core material**

Field ID	Rock Properties		Experimental Dataset	
	Brief lithological description	Strength	Type	Amount
A	Well Consolidated, Fine Grained Sandstones Interbedded with Thin Shale	Strong	slabbed core	13.3 ft
B	Moderately Consolidated, Fine Grained Sandstone and Shale	Medium to Strong	slabbed core	7.8 ft
C	Loosely Consolidated, Medium Grained Sandstone	Weak	plug sample	7 plugs

### **Terratek Scratch Test**

The Scratch Test was developed in the late 1990's at the University of Minnesota as a fast rock mechanical profiling technique to provide a strength index (Terratek Strength Index – TSI) that is positively correlated with UCS [2, 3, 4, and 5]. The Scratch Test consists of creating a continuous groove of constant depth on the surface of a rock sample at a constant velocity. The amplitude of the force acting on the cutter head are recorded continuously. An intrinsic specific energy parameter is sought throughout scratch testing which is a function of (a) the cutting process, (b) the inclination of the force acting on the cutting face, and (c) the friction coefficient across the cutter flat. Depending on rock type, mechanical properties, and cutter depth, the area of investigation and depth of damage will vary significantly. Also, the depth of cut impacts the type of failure process observed throughout testing, i.e., differing depths produce ductile and brittle failure. For ductile failure, the energy consumed is related to the volume of removed rock, while in the brittle mode, the energy consumed is related to the surface of the cracks while forming rock chips [6].

The scratch testing technique is based on a model of rock/cutter interaction in the ductile regime [7]. The model has four key assumptions: (1) the forces on the cutting face, which is suitably averaged over a long distance compared to the depth of the cut, is proportional to the cross-sectional area of the groove traced by the cutter, (2) the inclination of the average force on the cutting face is constant, (3) there is a frictional contact between the cutter flat and rock interface, and (4) the cutter wear is negligible.

### **Impulse Hammer Technique**

The Impulse Hammer probe used is integrated to a petrophysical core scanning system manufactured by New England Research. This system also allows for routine scanning of gas permeability, P- and S-wave velocity, electrical resistivity and infrared absorbance. The scanner platform, shown in Figure 1(a), can accommodate up to 12 feet of whole or slabbed core material at a time. The computer-controlled gantry system first maps the core surface with a laser to identify edges and fractures and exclude them from the measurement grid. Then the system can run automatically with no further operator assistance and map the selected physical properties according to the defined layout.

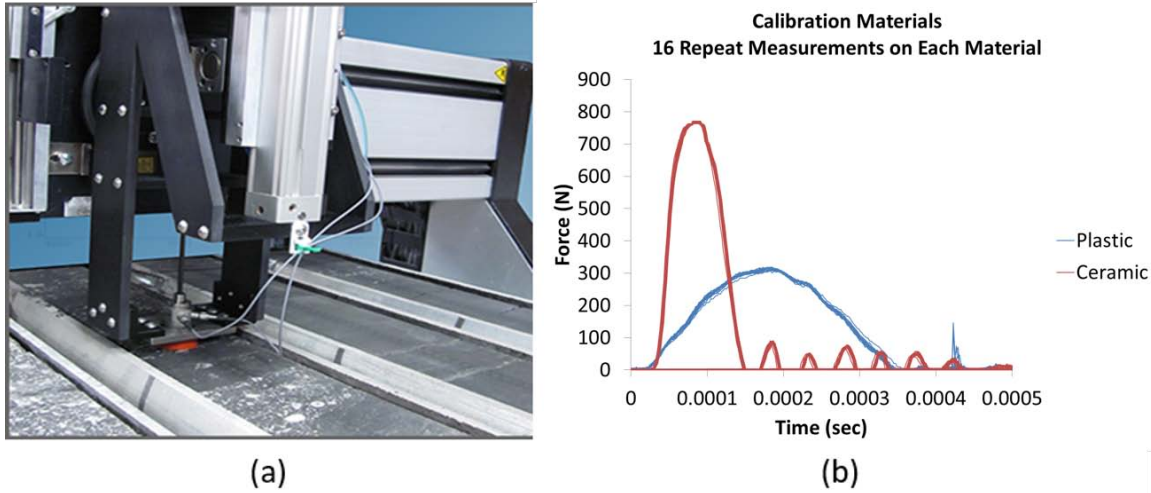


**Figure 1. (a) A photograph of the measurement platform used in this study, with several sample types on the table. (b) Example of the Impulse Hammer response on two different elastic materials. 16 repeat measurements are made on each sample, illustrating the level of repeatability.**

The Impulse Hammer was developed to provide a non-destructive mechanical profiling method. It was also designed to be fully automated for use on standard slabbed core without the need for special surface preparation. The area of investigation for the Impulse Hammer measurement is on the order of a millimeter and is commonly used with a measurement spacing of 2mm or greater depending on the application. Unlike more traditional rebound hardness techniques, the Impulse Hammer method can be used to extract both an elastic stiffness and a hardness index.

The measurement consists of dropping a mass equipped with a tip of known radius of curvature onto the core surface while continuously measuring the force applied at the tip at a very high sampling rate. A purely elastic Hertzian contact model is used to describe the impact of a sphere with an infinite sheet [8, 9]. The observed force-time function is fit to the model described in Equation (1).

$$f(t) \cong H \left( \frac{4}{3} \right) R^{\frac{1}{2}} \epsilon^* d^{\frac{3}{2}} \quad ; \quad d(t) \cong \sin \left( \frac{\pi(t-t_0)}{2T^*} \right) d_{\max} \quad (1)$$

where  $t$  is the time along the force-time function,  $R$  is the tip radius, and  $\epsilon^*$  is related to the tip properties and the reduced Young's modulus of the sample,  $E^*$ . The parameter  $H$  is a dimensionless hardness parameter, which for the case of elastic impact has a value of 1. The displacement-time function is approximated as shown in (1), where  $t_0$  is the time of impact.

$$d_{\max} = \left( \frac{15MV^2}{16R^2\varepsilon^*} \right)^{\frac{2}{5}} ; T^* = 2.94 \frac{d_{\max}}{2V} ; \frac{1}{\varepsilon^*} = \frac{(1-\nu_{\text{tip}}^2)}{E_{\text{tip}}} + \frac{1}{E^*} ; E^* = \frac{E}{(1-\nu^2)} \quad (2)$$

where, M is the mass of the impactor, V is the velocity of impact,  $\nu_{\text{tip}}$  is the Poisson's ratio of the tip,  $E_{\text{tip}}$  is the Young's modulus of the tip, and E and  $\nu$  are the material Young's modulus and Poisson's ratio of the test sample.

Thus the measured force-time function of impact is fit to elastic theory and allowed two free parameters,  $E^*$  and the impulse hardness parameter H, which can be related to the kinetic energy loss during impact.

Figure 1(b) shows several Impulse Hammer force-time functions for two different elastic materials, polyetherimide (plastic) and macor (ceramic). The plastic sample has a low Young's modulus and exhibits much lower force amplitude and longer period of indentation, while the ceramic sample has a high Young's modulus and provides a much higher force response in a relatively shorter time interval.

### **Procedures for Data Acquisition and Analysis**

In the following, only the procedures that pertain to the Impulse Hammer work performed at ALS are described:

For Fields A and B, where slabbed 1- and 2-foot long core sections were available,  $E^*$  was measured along the core axis at 5 mm spacing using NER's standard medium curvature tungsten carbide tip with  $R=3.8$  mm,  $E_{\text{tip}}=545$  GPa, and  $\nu_{\text{tip}}=0.23$ . All measurements were made using a fixed drop height of 12.5 mm and a total sensor mass of 69.7 grams, The data were processed using NER's default routine processing, yielding  $E^*$  and H. Due to different sampling rates and volume sensitivities for the Scratch Test and Impulse Hammer outputs, the comparison between TSI and  $E^*$  was initially carried out using histograms from common depth ranges.

For Field C, where original core sections were not available, RCA plugs were secured to the measurement table and mapped with the laser to delineate samples edges. A grid pattern of several measurements was performed on the end surface of every plug to provide a statistically representative data set. The data obtained were reduced by calculating average  $E^*$  values per plug and these were compared against TSI values from the parent core at the same depth.

It is worth noting that although the Scratch Test provides a finer length resolution than the Impulse Hammer, the volume effectively investigated by the Scratch Test itself is larger than the mm scale footprint of the Impulse hammer.

## RESULTS

### Fields A and B

Figure 2 shows a data set obtained on one of the core sections from Field A, together with a core photograph. The reduced Young's modulus and TSI values are plotted as a function of depth using two different vertical scales. The comparison demonstrates a visually good consistency between the two data sets, with some contrast in a few intervals. Also, note that locations where plugs had been taken could not be probed by the Impulse Hammer. In order to conduct a global comparison between the two data sets across a number of core sections studied, histograms were used, as shown in Figure 3. The same procedure was followed for all the core sections studied from Fields A and B. Some results are showed in Figures 4 and 5.

### Field C

Impulse Hammer data for Field C was obtained on RCA core plugs. Comparison between average  $E^*$  per plug and TSI obtained at the same location is listed in **Table 2**. In this case, the strength measured by both methods was much lower than for Fields A and B. Yet, reasonable correlation is observed between the two measurements.

**Table 2. Summary of Field C plug properties and test results.**

Plug ID	Gas K, md	Helium Porosity, % PV	TSI from core MPa	$E^*$ , GPa
1	278.	27.3	0.500	1.329
2	419.	28.8	1.500	0.833
3	742.	29.4	1.000	0.656
4	1290.	29.7	0.500	0.396
5	1140.	30.0	0.700	0.717
6	763.	27.5	0.400	0.561
7	1350.	28.3	0.600	0.361

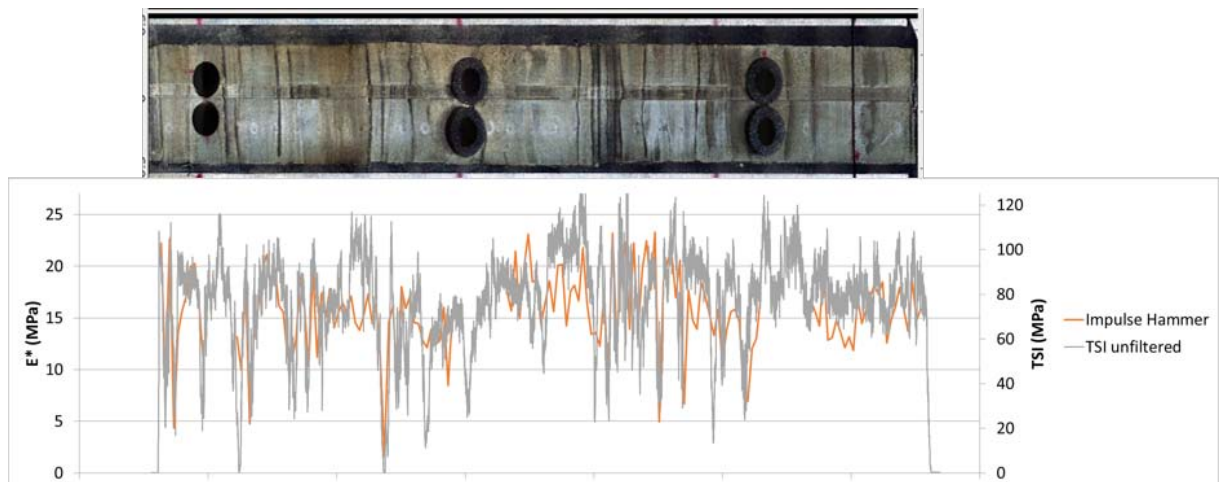


**Figure 2. Field A slabbed core photograph (above) and measured  $E^*$  and TSI values along the core length. This two foot interval consists of thin-bedded consolidated sand (tan color) and then shale (gray color). Note the sensitivity of both properties to variability in strength.**

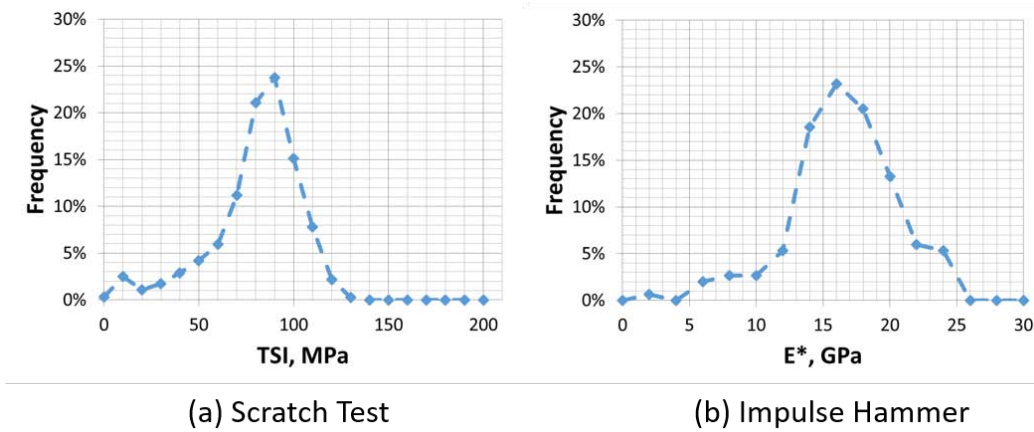


Figure 3. Field A: Histograms of all data showed in Figure 2. (a) TSI. (b) E\*.

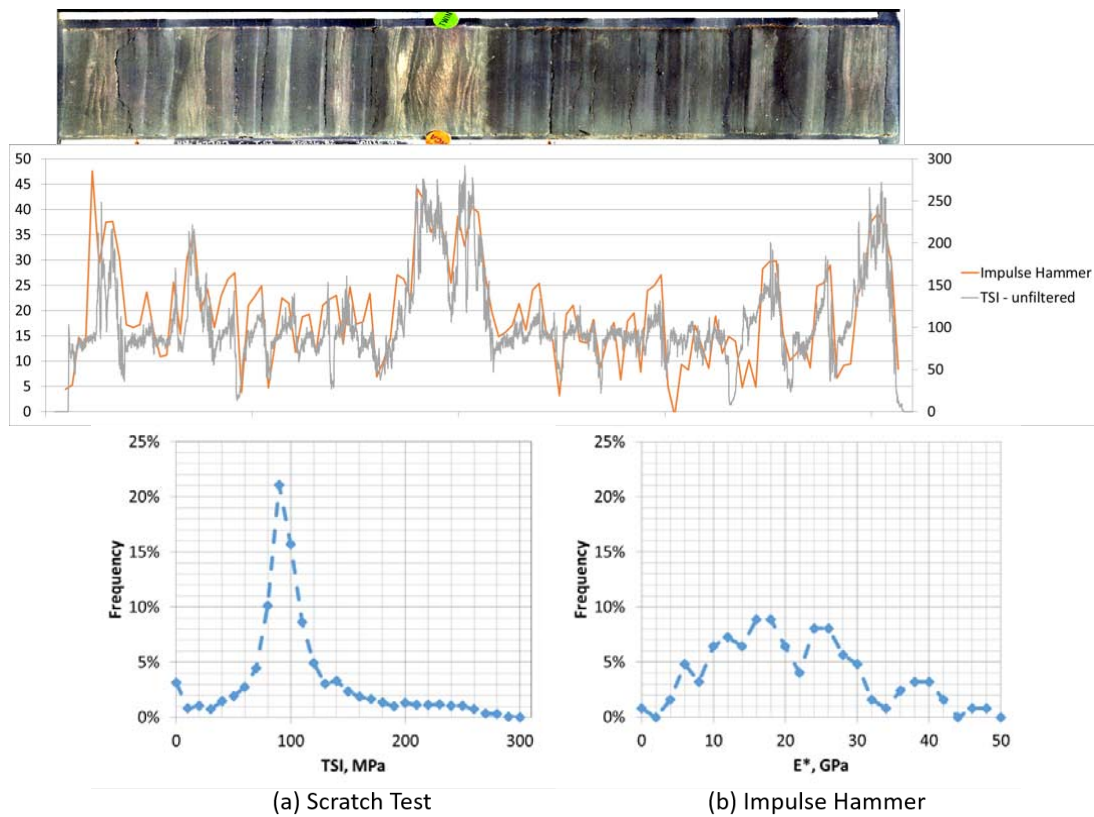
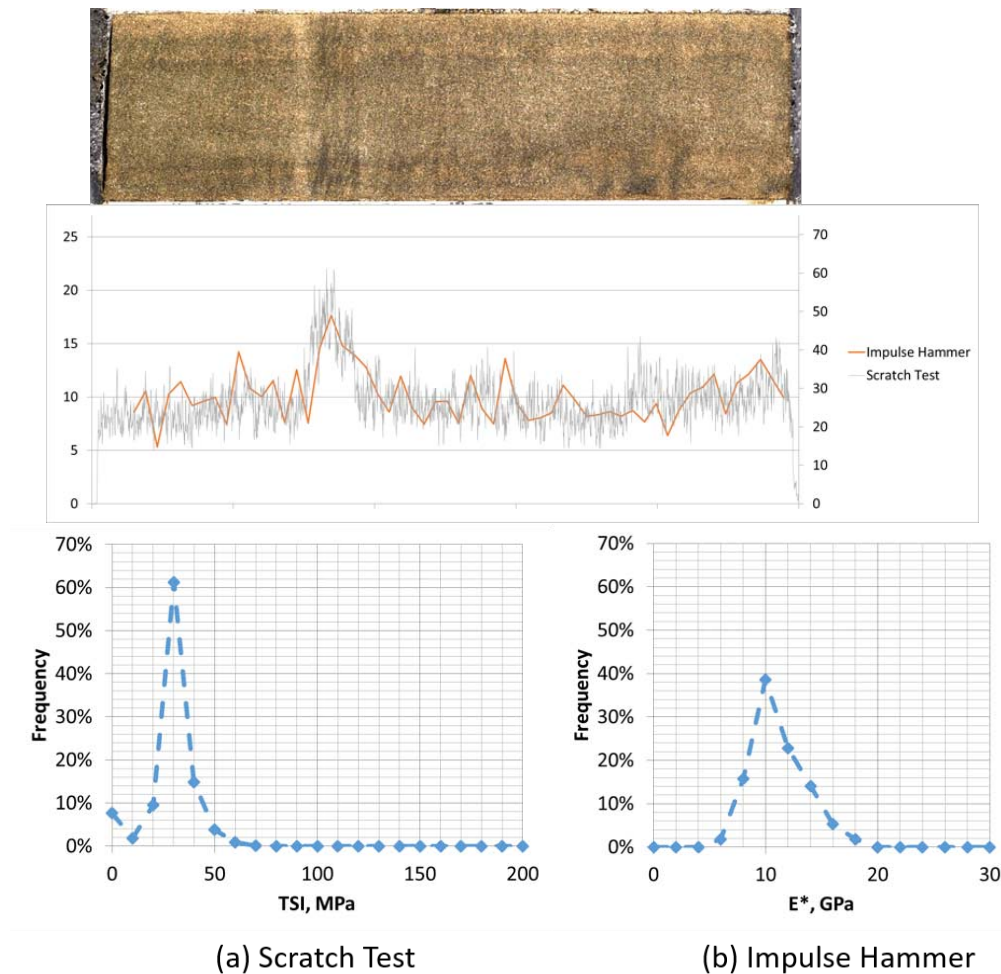


Figure 4. Field A slabbed core photograph and measured E\* and TSI values along the core length (above). This two foot interval consists of shale (gray color) and thin-bedded consolidated sand (tan color). The tan-colored cross-bedded sandstone exhibits substantially higher strength than the rest of the core per both methods. Below: Histograms for above data. (a) TSI. (b) E\*.



**Figure 5. Field B slabbled core photograph and measured  $E^*$  and TSI values along the core length (above). This one foot section consists of moderately consolidated sandstone. Relatively high strength interval associated with more bedded lithology is observed by both methods. Below: Histograms for above data. (a) TSI. (b)  $E^*$ .**

## DISCUSSION AND CONCLUSION

### Impulse Hammer as a TSI predictor

The data acquired and discussed in the previous section allows us to conduct a global comparison between the Scratch-Test-derived Terratek Strength Index (TSI) and the Impulse-Hammer-derived reduced Young's modulus  $E^*$ . Based on our observations on cores and data sets, all the measured sections were divided into several internally-homogeneous subsets to perform the comparison. For each of those subsets, a separate histogram of both TSI and  $E^*$  values was traced and the averages of those histograms were used as representative TSI- $E^*$  pairs for a global comparison. The result of this analysis is shown in **Table 3**. Note that in Field A some intervals display very similar pairs of average properties. In the case of Field C, each plug was considered as its own group.



**Table 3. Summary of results obtained from histogram analysis for each individual rock type with lithological description.**

Field	Length/ Quantity	Peak TSI, Mpa	Peak IH, Gpa	Comment
A	2 ft	70.000	16.000	sand w/shale laminae
A	3 ft	260.000	45.000	shale w/sand laminations
A	3 ft	70.000	16.000	massive sand
A	3 ft	40.000	6.000	Combination of silt and sand interbedded with shale laminae.
		90.000	16.000	
A	3 ft	10.000	2.000	Alteration of clean sand and silt with lower shale content
		60.000	14.000	
		70.000	16.000	
B	3 ft	40.000	6.000	shale
B	3 ft	10.000	4.000	massive sand
B	1 ft	60.000	18.000	massive sand
B	1 ft	30.000	10.000	massive sand
C	1 plug	2.000	1.200	sand
C	1 plug	1.500	0.833	sand
C	1 plug	1.000	0.656	sand
C	1 plug	0.500	0.396	sand
C	1 plug	0.700	0.717	sand
C	1 plug	0.400	0.561	sand
C	1 plug	0.600	0.361	sand

shale	sand
-------	------

The breakdown of Table 4 helps us to establish the global correlation between TSI and  $E^*$ , which is shown in Figure 8. The sands in Fields A, B and C appear to show very strong TSI- $E^*$  correlation. Best fitting power laws given below show similar factors and exponents:

$$\text{Field A sand: } TSI = 2.1226 E^{*1.263} \quad (3)$$

$$\text{Field B sand: } TSI = 1.9194 E^{*1.192} \quad (4)$$

$$\text{Field C sand: } TSI = 1.4131 E^{*1.159} \quad (5)$$

The shales from Fields A and B are fit with the polynomial:

$$\text{Field A and B shales: } TSI = -0.1786 E^{*2} + 8.9286 E^* - 7.1429 \quad (6)$$

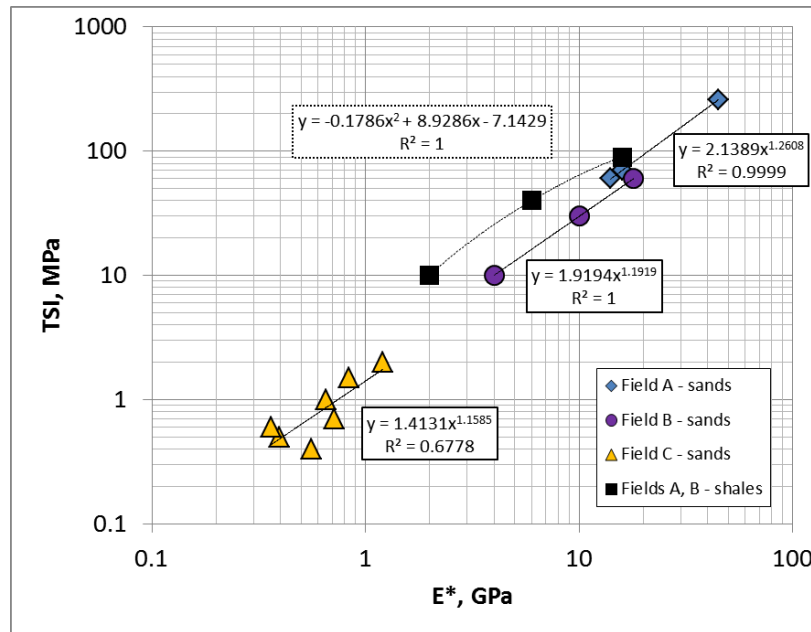


**Figure 6. Group-wise correlation between TSI and  $E^*$  with best fits per lithology**

The obtained fits show that the correlation between TSI and  $E^*$  for GoM sands is very good over a wide range of strengths. More complex mechanical behavior may explain the different trend observed in shale, although more data points might lead to finding a power law equally relevant.

Based on these results, we find that the TSI and  $E^*$  parameters are adequately comparable in representing the variations of mechanical properties along a given profile (as shown in Figures 3-5). In addition, those parameters are very consistent in their relationship of magnitude, especially in sands. This provides a comparatively attractive method as the impulse Hammer is non-destructive and provides independent measurements at mm scale.

### **Impulse Hardness H**

As described in the methods section, the Impulse Hammer produces an additional parameter which is sensitive to the permanent deformation experienced by the material during impact. This parameter, the impulse hardness, offers a more complete description of the mechanical behavior of the material during the test. The impulse hardness  $H$  operates in the numerical inversion as a scaling factor on the initial impact velocity and reflects the contrast between the velocities at impact and after rebound. Therefore, it correlates with another strength index known as the Leeb rebound hardness. Although  $H$  essentially allows to draw a more complete picture of the elasto-plastic mechanical response of the material during Impulse Hammer testing, it may also be used in the context of the present study to achieve a TSI prediction that does not necessitate the definition of rock types based on core observation. To explore that possibility, the data

set presented here was first reworked to allow for a one-to-one correspondence at each depth between TSI and pairs of  $E^*$  and  $H$  values. That was achieved by averaging the TSI data over entire Impulse Hammer depth spacings. Doing so, one can use the trends that were defined in Figure 6 to cross-plot the predicted TSI versus the measured TSI for all individual Impulse hammer data points. This comparison is shown in Figure 7a. Without changing anything to the results obtained using the histogram analysis, we observe that the predicted TSI values lie within a factor of two of the measured ones over three orders of magnitude. In Figure 7b, instead of using the rock types of Table 3, the impulse hardness was used to distinguish between two populations which can be loosely defined as sands and shales. As can be seen on the plot, this procedure leads to a very similar result, suggesting that in regard to the objective set here of recovering TSI values from Impulse Hammer measurement, the use of both  $E^*$  and  $H$  yields a result that is as satisfactory as the one of  $E^*$  and rock types defined from core observation.

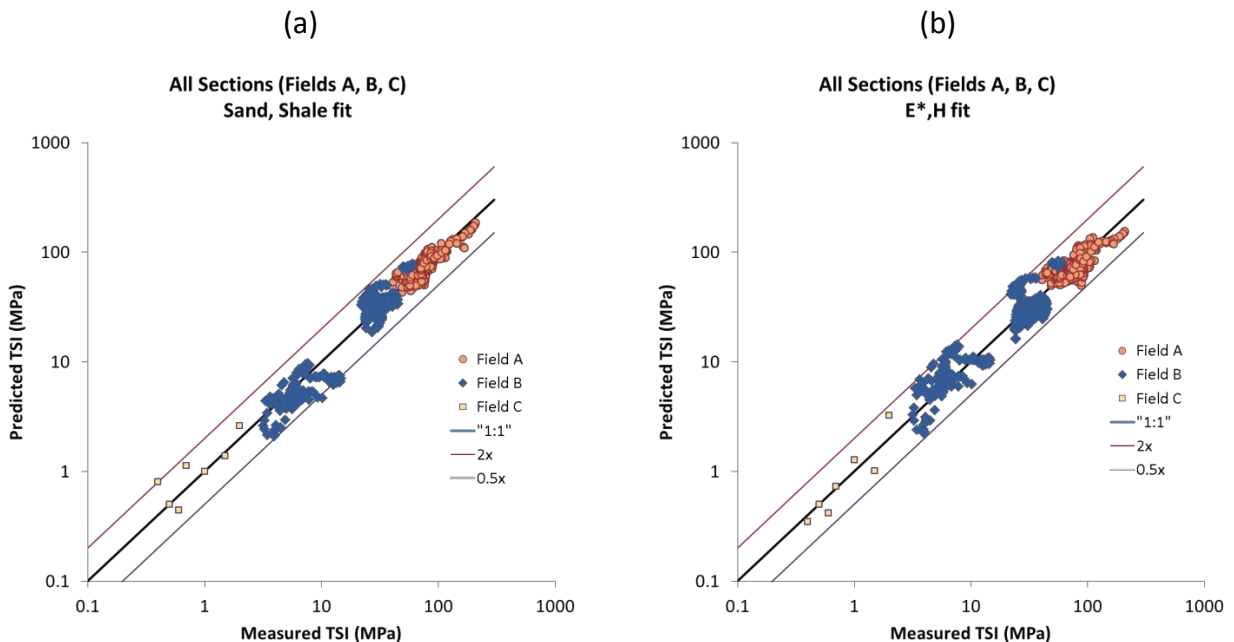


**Figure 7. Comparison between predictions realized using the Impulse hammer data. (a) Using the fits of Figure 6 which use a lithology-based separation. (b) With Impulse Hammer data only but using the hardness  $H$  as a rock type indicator.**

In conclusion, the trial conducted on various BP GoM core to validate the Impulse Hammer as a mechanical profiling tool can be considered successful as benchmarked against existing TSI data. Both rock-type specific and rock-type independent correlations are shown to fit the GOM dataset spanning 3 orders of magnitude in strength. It is worth noting here that this study implicitly assumes that the Scratch Test results are a representation of the variations that would be observed for uniaxial compressive strength data. Comparing the Impulse Hammer directly with UCS data, and extending the dataset to include a wider range of rock-types and compositions, could constitute another worthwhile validation step. Looking forward in time, it appears that Impulse Hammer

provides a more complete set of mechanical parameters that should therefore be tested against more complex data sets such as a combination of UCS and acoustic velocity in order to explore its potential for a wider applicability. Modifications to tip geometry and impact force are being explored as ways to characterize additional mechanical properties, including terms such as brittleness, tensile strength, and mechanical anisotropy.

### **ACKNOWLEDGEMENTS**

The authors would like to thank BP America, ALS Reservoir Laboratories, BHP Billiton Petroleum, Chevron, Conoco Phillips, Exxon, New England Research and Petrobras companies for permission to publish this work.

This paper reflects the views of the authors and does not necessarily reflect or represent those of their employing companies.

### **REFERENCES**

1. Chang, C., Zoback, M.D. et al. 2006. Empirical relations between rock strength and physical properties in sedimentary rocks. *Journal of Petroleum Science and Engineering*, **51**, 223-237.
2. Adachi J., and E. Detournay. 1996. Drescher A. Determination of rock strength parameters from cutting tests. *2nd North American Rock Mechanics Symposium*.
3. Detournay E., A. Drescher, P. Defourny, and D. Fourmaintraux. 1995. Assessment of rock strength properties from cutting tests: Preliminary experimental evidence. *Proc Of the colloquium Mundanum on Chalk and Shales*, Brussels. p. 11–3.
4. Detournay E, A. Drescher, and D.A. Hultman. 1997. Portable rock strength evaluation device. US Patent 5,670,711. U.S. Patent; 5, 670, 711.
5. Richard T, E. Detournay, A. Drescher, P. Nicodeme, and D. Fourmaintraux. 1998. The scratch test as a means to measure strength of sedimentary rocks. *SPE/ISRM EUROCK 98*.
6. Naeimipour, A., J. Rostami, E. Keller, O. Frough, S. Wang. 2015. Estimation of rock strength by means of scratch probe. 49th US Rock Mechanics/Geomechanics Symposium. San Francisco, California, 28 June-1 July.
7. Detournay E, and P. Defourny. 1992. A Phenomenological Model for the Drilling Action of Drag Bits. *Int J Rock Mech Min Sci Geomech Abstr*.
8. Rathbun, A.P., S.R. Carlson, R.T. Ewy, P.N. Hagin, C.A. Bovberg, G.N. Boitnott. 2014. Non-destructive impulse based index testing of rock core. 48th US Rock Mechanics/Geomechanics Symposium. Minneapolis, Minnesota, 1-4 June.
9. Johnson, K. 1985. *Contact Mechanics*. Cambridge: Cambridge University Press.